PHARMACEUTICAL BIOLOGY
2025, VOL. 63, NO. 1, 364–373
https://doi.org/10.1080/13880209.2025.2498166

Taylor & Francis
Taylor & Francis Group

RESEARCH ARTICLE

OPEN ACCESS Check for updates

Tanshinone IIA reduces tubulointerstitial fibrosis by suppressing GSDMD-mediated pyroptosis

Xueling Yang[a*], Qinglin Luo[a*], Zhifen Wu[a], Chunxuan Wang[a], Yuanjing Yang[a], Luquan Zheng[a], Ke Li[b], Lei Zhao[a¶] and Yang Jurong[a¶]

[a]Department of Nephrology, The Third Affiliated Hospital of Chongqing Medical University, Chongqing, China; [b]Core Research Laboratory, The Second Affiliated Hospital, Xi'an Jiaotong University, Xi'an, China

ABSTRACT

Context: Tanshinone IIA (Tan IIA), a bioactive compound derived from the traditional Chinese herb *Salvia miltiorrhiza (Family Lamiaceae, Authority Bunge)*, is well-known for its protective effects in various kidney diseases. However, its role in obstructive nephropathy has not been thoroughly investigated.

Objective: This study aimed to explore the protective effects of Tan IIA in a mouse model of unilateral ureteral obstruction (UUO) and to elucidate the cellular and molecular mechanisms underlying these effects.

Materials and methods: Gasdermin D (GSDMD) knockout mice and their wild-type (WT) littermates underwent UUO surgery, with Tan IIA treatment administered 24 h prior. Human proximal tubular cells (HK-2 cells) were treated with TGF-β1 to induce fibrosis (50 ng/mL for 24 h), followed by Tan IIA treatment (5 μM) for an additional 3 h.

Results: Tan IIA significantly reduced the expression of extracellular matrix (ECM) components, including collagen I, α-smooth muscle actin (α-SMA), vimentin and fibronectin, in UUO mice. Tan IIA attenuated GSDMD-mediated pyroptosis. However, in GSDMD knockout mice subjected to UUO, the protective effects of Tan IIA on ECM gene expression and collagen deposition in the tubular interstitium were reduced. *In vitro* studies showed that Tan IIA reduced GSDMD activation and fibronectin protein expression in HK-2 cells.

Discussion and conclusions: Tan IIA may mitigate GSDMD-mediated pyroptosis in renal tubular epithelial cells (RTECs) and reduce kidney fibrosis, highlighting its potential as a therapeutic strategy to prevent the progression of kidney disease after ureteral obstruction.

ARTICLE HISTORY

Received 7 August 2024
Revised 2 March 2025
Accepted 21 April 2025

KEYWORDS

Chinese herbal medicine; unilateral ureteral obstruction; cell death; chronic kidney disease; Gasdermin D; pyroptosis

Introduction

Renal fibrosis is a hallmark of obstructive nephropathy and a critical driver of the progression to chronic renal failure (Huang et al. 2023; Krukowski et al. 2023; Nørregaard et al. 2023). Obstructive nephropathy, characterized by kidney dysfunction and interstitial fibrosis, is primarily induced by urinary tract obstructions that can lead to chronic kidney disease (CKD) and, in severe cases, end-stage renal disease (ESRD) (Nørregaard et al. 2023). In the early stages, damaged renal tubular epithelial cells (RTECs) produce elevated pro-inflammatory and pro-fibrotic cytokines, chemokines, proteases and growth factors (Nørregaard et al. 2023). Activated RTECs can synthesize extracellular matrix (ECM) components such as fibronectin and collagen I, undergoing phenotypic alterations marked by loss of epithelial markers such as E-cadherin and upregulation of α-smooth muscle actin (α-SMA), resulting in a mesenchymal phenotype. These changes accelerate renal fibrosis and exacerbate the decline in kidney function (Ruiz-Ortega et al. 2020; Li H et al. 2022). Thus, alterations in RTECs serve as critical indicators of the progression of tubulointerstitial fibrosis (Ma et al. 2023).

Emerging evidence indicates that naturally derived compounds benefit various diseases (Ren et al. 2021; Kuang et al. 2023; Li J et al. 2023; Sun et al. 2023). Recent studies have shown that many compounds protect against tubulointerstitial fibrosis (Cao et al. 2022; Chang et al. 2022; Wang H et al. 2022; Lin et al. 2023). Tanshinone IIA (Tan IIA), a major active component of *Salvia miltiorrhiza (Family Lamiaceae, Authority Bunge)*, has been extensively investigated for its therapeutic potential in numerous conditions, including cardiovascular disease, cancer, diabetes, obesity and neurogenic disorders (Ansari et al. 2021; Miao et al. 2022; Yang et al. 2023). Tan IIA exerts its pharmacological effects mainly through anti-toxic, anti-inflammatory, anti-oxidative stress and anti-fibrotic activities (Zhang et al. 2022; Wu S et al. 2023). Studies have shown that Tan IIA ameliorates pyroptosis through multiple pathways, reducing the production of inflammatory mediators and alleviating tissue inflammation (Chai et al. 2023;

CONTACT Lei Zhao zhaoleitang@126.com; Jurong Yang 650230@hospital.cqmu.edu.cn Department of Nephrology, The Third Affiliated Hospital of Chongqing Medical University, Chongqing, China.
*Xueling Yang and Qinglin Luo contributed equally to this work.
¶Lei Zhao and Yang Jurong share senior authors.
Supplemental data for this article can be accessed online at https://doi.org/10.1080/13880209.2025.2498166.

Song et al. 2023). Furthermore, previous research has shown that Tan IIA can mitigate kidney injury by alleviating oxidative stress, reducing inflammation and attenuating renal fibrosis (Dou et al. 2022; Wu Q et al. 2023). However, it remains unclear whether Tan IIA specifically attenuates pyroptosis in renal parenchymal cells during kidney injury and consequently hinders the progression of renal fibrosis.

Pyroptosis is a recently identified form of programmed inflammatory cell death characterized by releasing inflammatory factors, lysosomal enzymes and other cellular contents (Fu et al. 2022; Gao et al. 2022; Yang et al. 2022; Jin et al. 2023). This process is primarily mediated by members of the Gasdermin family, especially Gasdermin D (GSDMD) and GSDMDE. Among these, GSDMD-dependent pyroptosis has been extensively studied. The activation of cysteinyl aspartate-specific proteinase (Caspase) 1 or Caspase 11/4/5 cleaves GSDMD, allowing the GSDMD N-terminus to translocate to the cell membrane and form pores, leading to the release of inflammatory factors such as IL-1β and IL-18 (Elias et al. 2023; Sanz et al. 2023). Pyroptosis plays a crucial role in the onset and progression of various kidney diseases (Li et al. 2021; Zheng et al. 2022), significantly affecting kidney function and severity of injuries by affecting tubular epithelial and inflammatory cells and influencing disease prognosis (Deng et al. 2021). Our previous studies have shown that GSDMD-dependent pyroptosis mediates the development of ischemia-reperfusion and septic acute kidney injury (AKI) (Yang et al. 2014; Deng et al. 2021). However, the role of pyroptosis in fibrosis progression remains poorly understood.

This study aimed to evaluate the protective effects of Tan IIA in a murine model of unilateral ureteral obstruction (UUO) and to elucidate the cellular and molecular mechanisms underlying its protective effects. Our findings demonstrated that Tan IIA treatment significantly reduced kidney fibrosis by inhibiting GSDMD-mediated pyroptosis in RTECs and suppressing excessive ECM deposition, contributing to its protective effects.

Materials and methods

Materials and reagents

The materials used were as follows: Tanshinone IIA (HY-N0135, purchased from MedChemExpress, China); Peroxidase AffiniPure Goat Anti-Rabbit IgG (H + L) (33101ES60, Yeasen Biotech, Shanghai, China); polyclonal rabbit anti-mouse Cleaved Caspase-1 (89332), NLRP3 (15101), collagen I (72026), vimentin (5741) and mouse anti-mouse IL-1β (12242) (all from Cell Signaling Technology, Danvers, USA); polyclonal rabbit anti-mouse GSDMD (ab219800), fibronectin (ab2413) and α-SMA (ab124964) (all from Abcam, Cambridge, UK); 4′,6-diamidino-2-phenylindole (DAPI, Life Sciences, Paisley, UK); Lens culinaris agglutinin (LCA, Vector Laboratories, Peterborough, UK); TRIzol reagent, PrimeScript™ RT Master Mix (TKR-RR036B) and TB Green® Premix Ex Taq™ II (TKR-RR820B) (all from Takara Biotechnology, Tokyo, Japan); fetal bovine serum (FBS, GIBCO BRL, Rockville, MD, USA); M-PER mammalian protein extraction reagent, BCA protein assay kit, RIPA lysis buffer and Protease and Phosphatase Inhibitor Mini Tablets (A32961) (all from Thermo Fisher, Waltham, USA). Antibodies information is provided in Supplementary File 1.

Animal models

GSDMD knockout mice on a C57BL/6 (B6) background were generously provided by Prof. Limin Lu (Fudan University, China) and bred at Chongqing Medical University. Wild-type (WT) littermates were used as GSDMD$^{-/-}$ mice controls. The murine model of UUO, which mimics urinary tract obstruction and subsequent kidney damage leading to renal fibrosis, was established in both WT and GSDMD$^{-/-}$ male mice (8–12 weeks old). Mice were treated with Tan IIA or vehicle control. Under general anesthesia induced by intraperitoneal injection of pentobarbital (75 mg/kg), mice in the UUO group underwent left ureter ligation. Sham-operated mice underwent ureteral exposure without ligation, following a procedure previously described (Fan et al. 2023). The Tan IIA-treated group received daily intraperitoneal injections of Tan IIA (20 mg/kg) beginning 24 h before the UUO operation. In contrast, the vehicle control group received 10% dimethyl sulfoxide in PBS daily (Jiang et al. 2015). Mice were kept under specific pathogen-free conditions and sacrificed at predetermined time points. This experiment was approved by the Ethics Review Committee for Animal Experimentation at Chongqing Medical University (approval code: IACUC-CQMU-2024-0164, approved on 4 March 2024). This approval encompasses three experiments, as the study is part of a larger research initiative that may lead to multiple related publications under a single overarching Ethics Approval.

HK-2 cells culture and treatment

Human proximal tubular cells (HK-2 cells) were obtained from the National Collection of Authenticated Cell Cultures (species: Homo sapiens; CVCL numbers: CVCL_0302; catalog numbers: SCSP-511) and cultured in DMEM/F-12 medium supplemented with 10% fetal bovine serum and 1% penicillin-streptomycin. After three passages, HK-2 cells were induced to undergo fibrosis by treatment with TGF-β1 (up to 50 ng/mL) for 24 h at 37 °C, followed by Tan IIA treatment (5 μM) for an additional 3 h (Cao et al. 2017).

HK-2 cells were transfected with GSDMD-specific or control siRNA 16 h before stimulation assays for specific experiments. Cells grown in 6-well plates were treated with siRNA oligomers complexed with Lipofectamine 3000 reagent (Invitrogen). The GSDMD siRNA sequences were siRNA3: GGAACUCGCUAU CCCUGUUTT (sense) and AACAGGGAUAGCGAGUUCCTT (antisense). Transfection efficiency was confirmed by Western blot analysis (Figure 5e).

Assessment of renal fibrosis

Kidney paraffin sections (4 μm) were stained with Masson's Trichrome to assess kidney fibrosis. Three to four random fields of view (at 200× magnification) were selected to calculate the percentage of collagen deposition and compare renal interstitial fibrosis among different groups.

Immunohistochemistry

Before staining, kidney sections (4 μm) were deparaffinized and rehydrated. The sections were incubated with 3% H_2O_2 to quench endogenous peroxidase activity. The sections were incubated overnight at 4 °C with primary antibodies specific for collagen I (1:200), α-SMA, vimentin (1:1000), vimentin (1:200) or GSDMD (1:5000) and subsequently incubated with a secondary antibody at 37 °C for 30 min. The sections were stained with DAB, and the nuclei were counterstained with hematoxylin. The degree of positive staining was analyzed using ImageJ software. Two

independent experts evaluated all tissue sections in a double-blind manner.

Western blot

Mouse kidney tissue lysates were prepared using RIPA buffer with a cocktail of phosphatase and protease inhibitors on ice, while cell lysates were prepared using M-PER under the same conditions. The protein concentration was measured using the BCA protein assay kit, following the manufacturer's instructions. Equal amounts of protein (80 μg per lane) were separated by SDS-PAGE and transferred to a PVDF membrane. Membranes were blocked with 5% BSA for 1 h and incubated overnight with primary antibodies (dilution:1:1000). The membranes were incubated with HRP-conjugated secondary antibodies (dilution:1:5000). Protein bands were visualized using Amersham ECL Select™ detection reagent (GE Healthcare Life Sciences, USA). Relative amounts of GSDMD, GSDMD-N, collagen I, α-SMA, vimentin, fibronectin, IL-1β, IL-18, NLRP3 and Caspase 1 were quantified by normalizing to β-actin.

Quantitative and conventional RT-PCR

Total RNA from fresh kidney tissue and HK-2 cells was extracted using TRIzol reagent and reverse-transcribed into cDNA. Real-time PCR was conducted on a Step One™ real-time PCR machine (Thermo Fisher, Waltham, MA, USA) using Fast SYBR® Green Master Mix. Relative gene expression was analyzed using the $2^{-\Delta\Delta CT}$ method, normalizing to β-actin and appropriate controls (Li et al. 2017). Primer sequence information is provided in Supplementary File 2.

Statistical analysis

Data are presented as mean ± SD. Comparisons between means of independent samples were conducted using a t-test, a one-way ANOVA, or a two-way ANOVA with a multiple comparison test. Data were analyzed using GraphPad Prism, version 9 (GraphPad Software, La Jolla, CA, USA). A p-value of <0.05 was considered statistically significant.

Results

Tan IIA ameliorated renal tubulointerstitial fibrosis in the UUO mice model

Renal interstitial fibrosis is a hallmark of obstructive nephropathy. B6 mice were treated with Tan IIA (20 mg/kg daily intraperitoneal (i.p.) injection starting one day before UUO operation) or a vehicle control to evaluate its potential anti-fibrotic effects. Masson's Trichrome staining revealed a significant decrease in positive staining in Tan IIA-treated mice compared to the vehicle control group, indicating a reduction in ECM accumulation within the tubulointerstitial region (Figure 1a and 1b). This finding was further supported by Western blot analysis of kidney tissue lysates, which showed decreased levels of ECM proteins (α-SMA, vimentin, collagen I and fibronectin) in the Tan IIA group compared to controls (Figure 1c and 1d). Immunohistochemistry confirmed these results, showing a reduced deposition of collagen I, vimentin and α-SMA in the kidneys of Tan IIA-treated mice compared to the vehicle control group (Figure 2a-2c). These results suggest that Tan IIA effectively reduces interstitial fibrosis in WT mice after UUO surgery.

GSDMD deficiency reduced tubulointerstitial fibrosis in UUO mice model

Pyroptosis, a form of programmed cell death, has emerged as a key contributor to renal inflammation and fibrosis, although its precise role in fibrosis progression remains unclear. Whether Tan IIA mitigates UUO-induced renal fibrosis by inhibiting pyroptosis also requires further investigation. GSDMD cleavage by Caspases is essential for pyroptosis (He et al. 2015; de Vasconcelos et al. 2019). Our study first examined the expression and activation of GSDMD in the UUO model. Western blot analysis revealed significant GSDMD activation, evidenced by the cleaved form, GSDMD-N and IL-1β release in the kidneys 10 days after UUO, compared to sham-operated controls. Notably, GSDMD activation and IL-1β release were markedly reduced in GSDMD$^{-/-}$ mice (Figure 3a and 3b).

We then investigated the role of GSDMD in UUO-induced fibrosis by comparing GSDMD$^{-/-}$ and WT mice. Masson Trichrome and Sirius Red (SR) staining demonstrated substantial tubulointerstitial fibrosis in the kidneys of WT mice 10 days after UUO, which was significantly attenuated in GSDMD$^{-/-}$ mice (Figure 3c-3f). RT-PCR analysis revealed substantially lower intrarenal expression of ECM-related genes (α-SMA, collagen I and fibronectin) in GSDMD$^{-/-}$ mice compared to WT mice (Figure 3g). Additionally, Western blot analysis of kidney tissue lysates confirmed reduced levels of α-SMA and vimentin in GSDMD$^{-/-}$ mice compared to WT controls (Figure 3h and 3i). These findings strongly suggest that GSDMD-mediated pyroptosis plays a crucial role in fibrosis progression after ureteral obstruction.

Tan IIA treatment reduced renal pyroptosis in UUO mice

Tan IIA treatment has been reported to mitigate pyroptosis through multiple pathways (de Vasconcelos et al. 2019; Chai et al. 2023; Song et al. 2023). To investigate whether Tan IIA inhibits pyroptosis in the kidneys under UUO conditions, we analyzed GSDMD activation in renal tissues. Our results demonstrated that Tan IIA treatment significantly reduced the protein levels of the cleaved GSDMD-N form, as observed by Western blotting and immunohistochemical staining (Figure 4a and 4c). Furthermore, NLRP3 protein expression levels and the active form of Caspase 1, responsible for GSDMD cleavage, decreased markedly after Tan IIA treatment, as shown by Western blot analysis (Figure 4a and 4b). We also assessed IL-1β, a key inflammatory factor released during pyroptosis, using Western blotting, which revealed a significant reduction in IL-1β levels in the kidneys of UUO mice treated with Tan IIA (Figure 4a and 4b). These findings indicate that Tan IIA treatment effectively suppresses NLRP3-Caspase 1-mediated GSDMD cleavage, alleviating renal pyroptosis and inflammation.

Tan IIA treatment did not improve UUO-induced renal fibrosis in GSDMD$^{-/-}$ mice

To further investigate whether Tan IIA exerts its protective effects against UUO by targeting GSDMD-mediated pyroptosis, we evaluated its impact on renal fibrosis in GSDMD$^{-/-}$ mice. Masson's Trichrome staining revealed only minimal reductions in collagen

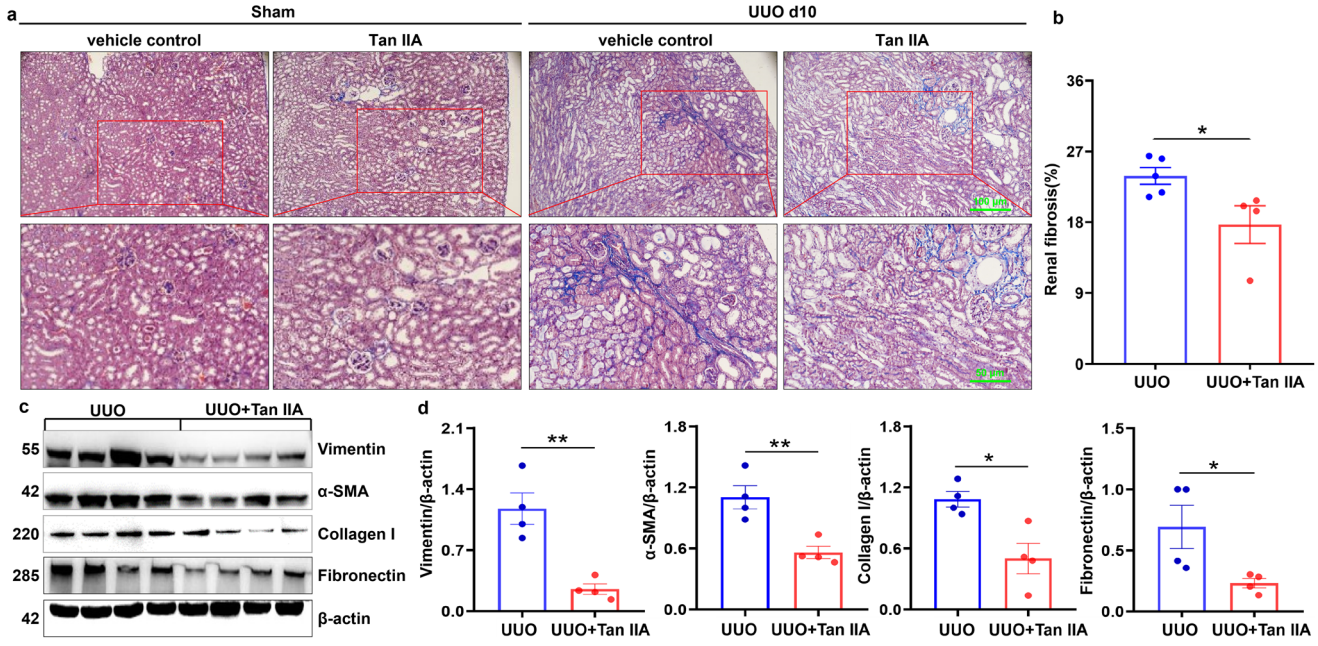

Figure 1. Tan IIA ameliorated renal tubulointerstitial fibrosis in the UUO mice model.
Unilateral ureteral obstruction (UUO) was induced in mice treated with Tanshinone IIA (Tan IIA) or vehicle control, and kidney samples were collected on day 10 after UUO surgery. (a) Representative images of Masson Trichrome (MT) staining show extracellular matrix (ECM) deposition in different groups. (b) Quantification of MT-stained areas (% of total area) in kidney tissues from the UUO and UUO+Tan IIA groups (n = 5). (c) Protein expression levels of fibronectin, α-smooth muscle actin (α-SMA), collagen I, and vimentin in the UUO and UUO+Tan IIA groups. (d) Quantitative analysis of fibronectin, α-SMA, collagen I, and vimentin protein expressions (normalized to actin) in the UUO and UUO+Tan IIA groups (n = 4). (b and d). Each dot represents an individual mouse. Data were analyzed using an unpaired t-test. *$p<0.05$, **$p<0.01$.

deposition in the kidneys of Tan IIA-treated GSDMD$^{-/-}$ mice compared to those treated with vehicle control (Figure 5a). Western blot analysis showed no significant differences in the fibrotic markers α-SMA and collagen I expression levels between the two groups (Figure 5b and 5c). These findings suggest that Tan IIA treatment did not significantly alleviate fibrosis in GSDMD$^{-/-}$ mice. This indicates that its anti-fibrotic effects in UUO are primarily mediated by inhibiting GSDMD-dependent pyroptosis.

Tan IIA inhibited cell pyroptosis and reduced the production of fibrotic markers in RTECs

RTECs are crucial resident cells in the kidneys that play a significant role in the fibrotic progression of kidney diseases. To investigate the effects of Tan IIA on RTECs, we treated HK-2 cells with TGF-β1, a primary inducer of renal fibrosis. Western blot, RT-qPCR analysis and immunofluorescence revealed that TGF-β1 markedly upregulated the expression of fibrotic markers (fibronectin, vimentin and collagen I) and pro-inflammatory cytokines (IL-1β and IL-18) (Figure 6a, 6b and 6e). However, pre-treatment with Tan IIA significantly reduced these increases, with a confirmed effect observed at 5 μM (Figure 6b, 6c and 6d). These results suggest that Tan IIA may alleviate the production of pro-inflammatory and fibrotic markers in RTECs by inhibiting GSDMD-dependent pyroptosis.

To further explore this hypothesis, we established GSDMD knockdown cells using siRNA. Western blot analysis showed that in GSDMD knockdown cells, TGF-β1 stimulation led to minimal increases in fibronectin, GSDMD-N, IL-18 and IL-1β protein levels. Tan IIA treatment did not significantly reduce these protein levels in knockdown cells (Figure 6e and 6f). These findings suggest that Tan IIA inhibits GSDMD-mediated pyroptosis and reduces the synthesis of fibrotic markers in RTECs, and this effect is dependent on GSDMD-mediated pyroptosis.

Discussion

Renal fibrosis is a hallmark of CKD, driven by various insults, including ureteral obstruction, leading to significant changes in renal hemodynamics and metabolic processes (Yuan et al. 2022; Wang YN et al. 2023; Miao et al. 2024). These changes profoundly impact RTECs, triggering responses such as partial epithelial-mesenchymal transition (EMT), cell cycle arrest, cellular senescence and apoptosis (Kalantar-Zadeh and Li 2020; Ruiz-Ortega et al. 2020; Nørregaard et al. 2023) These cellular responses increase the secretion of pro-inflammatory and pro-fibrotic cytokines, including TGF-β, connective tissue growth factor, IL-1β, IL-18 and IL-6 (Roccatello et al. 2024), which are crucial in the development of tubulointerstitial fibrosis (Tang et al. 2019; Wozniak et al. 2021; Li H et al. 2022). Given the essential role of RTECs in maintaining kidney function, their dysfunction accelerates CKD progression. Pyroptosis, an inflammatory form of programmed cell death (Wang JL et al. 2023; Zhao et al. 2023), has become a key mechanism contributing to renal fibrosis (Lan 2022; Liu et al. 2022; Wan et al. 2022; Wang F et al. 2022). GSDMD, a primary mediator of pyroptosis, is expressed in various cell types, including RTECs, and plays a pivotal role in kidney diseases (Wu J et al. 2021; Baatarjav et al. 2022). We showed that Tan IIA significantly reduced renal fibrosis in UUO-induced mice by inhibiting pyroptosis, specifically by suppressing the NLRP3-Caspase 1-GSDMD pathway in RTECs. These findings suggest that targeting pyroptosis could represent a promising therapeutic strategy for obstructive nephropathy.

Traditional Chinese medicines have long been used to treat renal diseases (Hu et al. 2022; Shao et al. 2023; Zou et al. 2023;

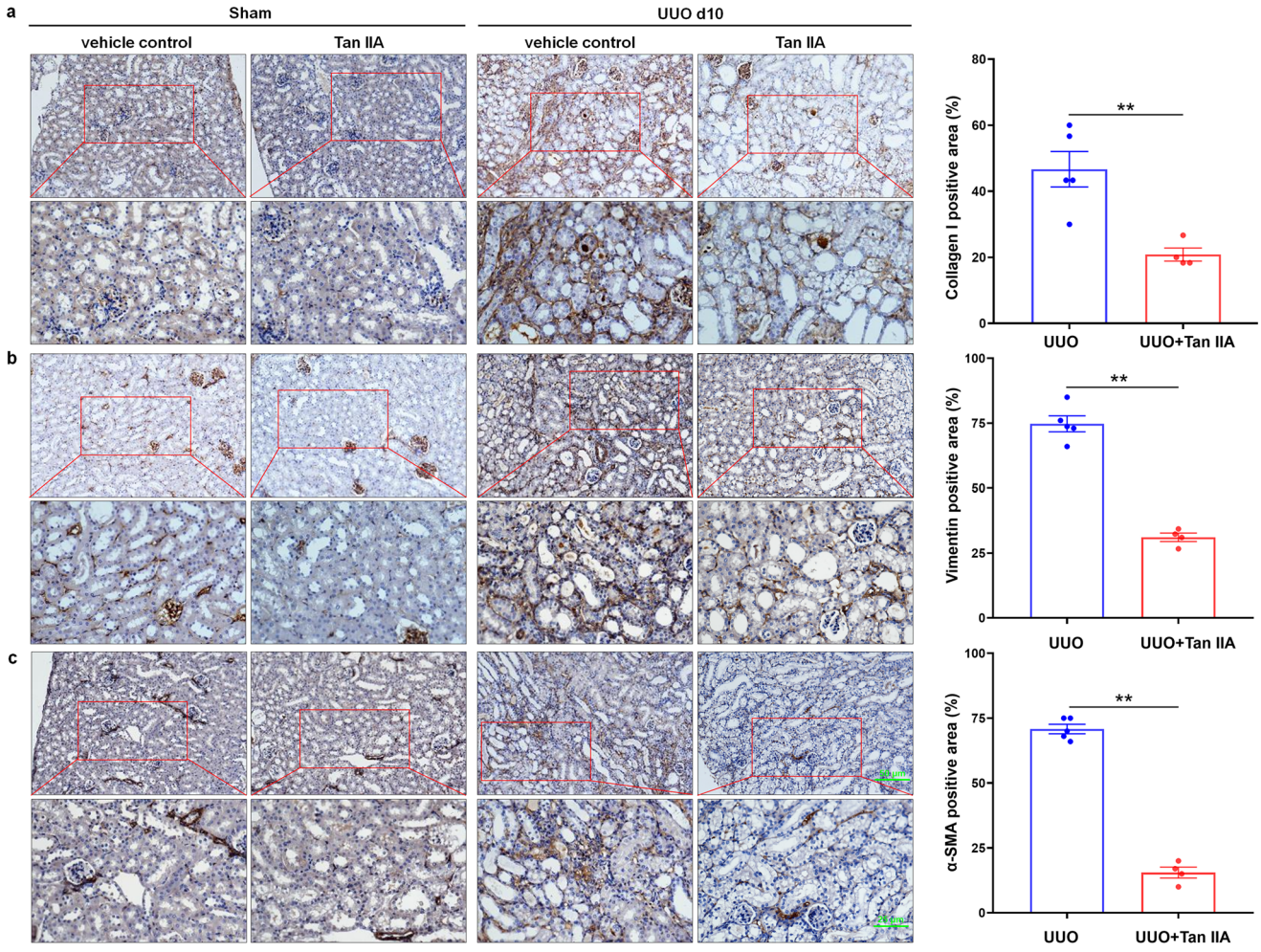

Figure 2. Tan IIA reduced renal protein expression levels of ECM in the UUO mice model.
UUO was induced in mice treated with Tanshinone IIA (Tan IIA) or vehicle control, and kidney samples were collected on day 10 after UUO surgery. (a-c) Immunohistochemical analysis of collagen I (a), vimentin (b), and α-SMA (c) in the UUO and UUO+Tan IIA groups (n = 5). (a-c). Each dot represents an individual mouse. Data were analyzed using an unpaired t-test. $^{**}p < 0.01$.

Guo et al. 2025; Wang et al. 2024). Tan IIA, a bioactive compound derived from the root of *Salvia miltiorrhiza* (commonly known as Danshen), is well-known for its cardioprotective effects (Li S et al. 2023) and is increasingly recognized for its renoprotective and anti-fibrotic properties (Dou et al. 2022). Previous research has shown that Tan IIA can reduce fibrosis by targeting the TGF-β1/Smad signaling pathway in a rat model of 5/6 nephrectomy and alleviate folic acid-induced fibrosis by lowering inflammation, characterized by decreased infiltration of inflammatory cells and expression of chemokines in mice (Wang et al. 2015; Jiang et al. 2016). We confirm that Tan IIA significantly alleviated UUO-induced fibrosis, as evidenced by reduced ECM deposition and lower expression of fibrotic markers, highlighting its therapeutic potential in managing renal fibrosis after UUO.

Pyroptosis, mediated by GSDMD cleavage, is crucial in tissue inflammation (Aglietti and Dueber 2017; Shi et al. 2017; Xue et al. 2019; Coll et al. 2022; Dubyak et al. 2023; Chen et al. 2024). Tan IIA has shown promise in alleviating NLRP3-Caspase 1-GSDMD-mediated pyroptosis in various tissues, including the brain, myocardial tissue and kidneys. Recent studies suggest that Tan IIA mitigates pyroptosis through the TLR4/NF-κB p65 pathway, reducing endoplasmic reticulum and oxidative stress (Li Y et al. 2022; Chai et al. 2023; Wu Q et al. 2023). In our UUO model, Tan IIA effectively suppressed NLRP3 inflammasome activation and subsequent Caspase 1 cleavage, resulting in lower GSDMD-N levels and reduced secretion of IL-1β. This reduction in pyroptosis was associated with a decrease in fibrotic marker levels, highlighting the role of GSDMD in promoting fibrosis in obstructed kidneys. Importantly, Tan IIA treatment did not significantly affect fibrosis progression in GSDMD$^{-/-}$ mice, reinforcing that its anti-fibrotic effects are primarily mediated by inhibiting GSDMD-dependent pyroptosis.

Previous studies have highlighted that kidney-infiltrating inflammatory cells undergo pyroptosis, contributing to tissue inflammation and fibrosis following UUO. Wang et al. reported that UUO induces GSDMD activation in neutrophils, resulting in the formation of GSDMD-dependent neutrophil extracellular traps (NETs). This process amplifies the production of inflammatory cytokines and increases α-SMA expression in macrophages through activation of the TGF-β1/Smad pathway, promoting renal fibrosis (Wu M et al. 2021; Wang Y et al. 2022). We observed a significant up-regulation of GSDMD-N expression in HK-2 cells treated with TGF-β1, indicating that TGF-β1 induces pyroptosis in RTECs. Furthermore, Tan IIA treatment markedly reduced TGF-β1-induced expression of fibronectin, collagen I and GSDMD-N in RTECs. Consistent with our *in vivo* findings, GSDMD knockdown in HK-2 cells significantly alleviated fibrosis, suggesting the role of pyroptosis in this process. However,

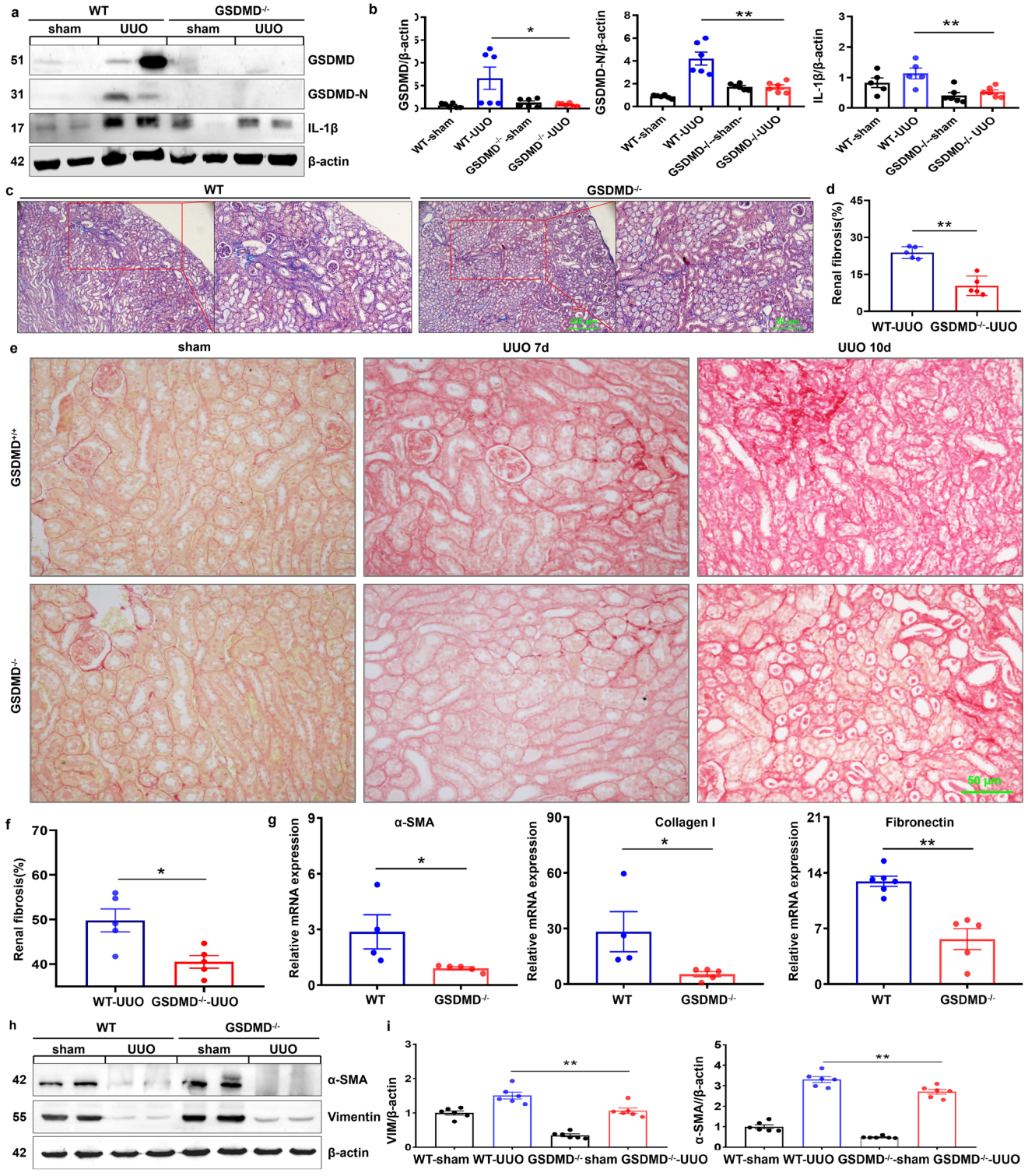

Figure 3. GSDMD deficiency reduced tubulointerstitial fibrosis in UUO mice model.
UUO was induced in wild-type (WT) and Gasdermin D (GSDMD)−/− mice, and kidney tissues were collected on days 7 and 10 after UUO surgery. (a) Protein expression levels of GSDMD, its cleaved form (GSDMD-N), and IL-1β in kidney tissues across different groups at day 10 post-UUO. (b) Quantitative analysis of GSDMD, N-GSDMD, and IL-1β protein expressions in various groups (n = 6). (c, e) Representative images of Masson Trichrome (MT) (c) and Sirius Red (SR) (e) staining, showing ECM deposition in kidney tissues from different groups. (d, f) Quantification of MT (d) and SR (f) stained areas in kidney tissues at day 10 after UUO in WT and GSDMD−/− groups (c and e) (n = 5). (g) Relative mRNA levels of fibronectin, α-SMA, and collagen I in WT and GSDMD−/− mice at day 10 after UUO (n = 5). (h) Protein expression levels of α-SMA and vimentin in kidney tissues from WT and GSDMD−/− mice at day 10 after UUO. (i) Quantitative analysis of α-SMA and vimentin protein expressions in WT and GSDMD−/− groups (n = 6). (b, d, f, g, i). Each dot represents an individual mouse. Data were analyzed using an unpaired t-test. $^{*}p < 0.05$; $^{**}p < 0.01$.

Tan IIA further reduced fibronectin levels in GSDMD knock-down HK-2 cells treated with TGF-β1, implying that additional cell death pathways may also be involved in fibrosis. Our findings demonstrate that Tan IIA reduces fibrosis by inhibiting pyroptosis and ECM production in RTECs, highlighting its potential as a therapeutic agent for obstructive nephropathy.

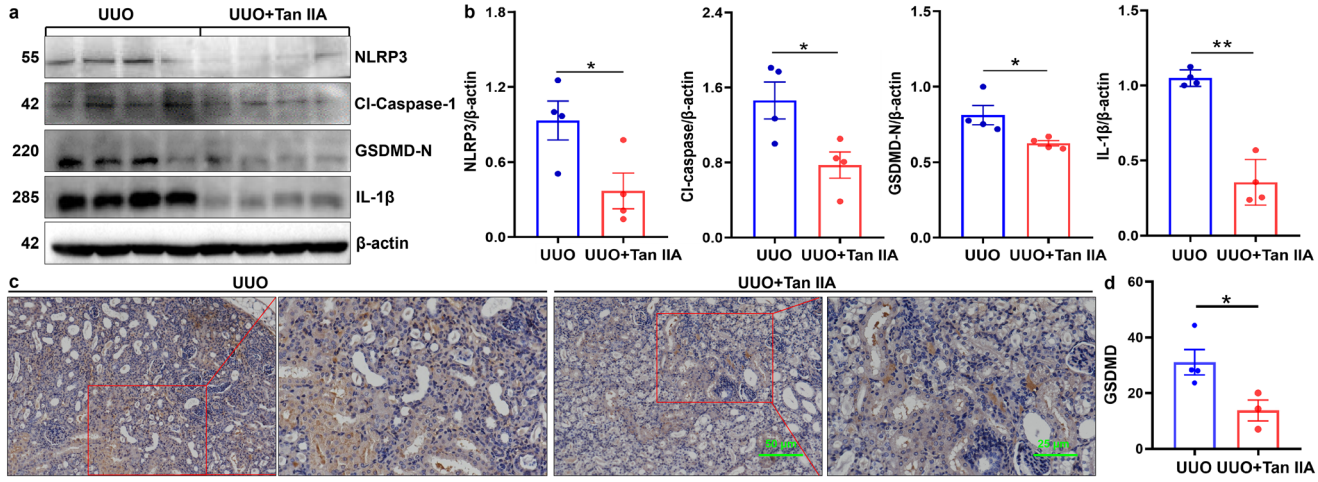

Figure 4. Tan IIA treatment reduced renal pyroptosis in UUO mice.
UUO was induced in mice treated with Tanshinone IIA (Tan IIA) or vehicle control, and kidney samples were collected on day 10 after UUO surgery. (a) Protein expression levels of NLRP3, cleaved Caspase 1 (Cl-Caspase 1), Gasdermin D (GSDMD)-N, and IL-1β in the UUO and UUO+Tan IIA groups. (b) Quantitative analysis of NLRP3, Cl-Caspase 1, GSDMD-N, and IL-1β protein expressions in the UUO and UUO+Tan IIA groups (n = 4). (c) Representative microscopy images of immunohistochemical staining for total GSDMD in the UUO and UUO+Tan IIA groups. (d) Quantitative analysis of GSDMD+ cells, determined by counting the number of positively stained cells (n = 5). (b, d) Each dot represents an individual mouse. Data were analyzed using an unpaired t-test. $*p < 0.05$; $**p < 0.01$.

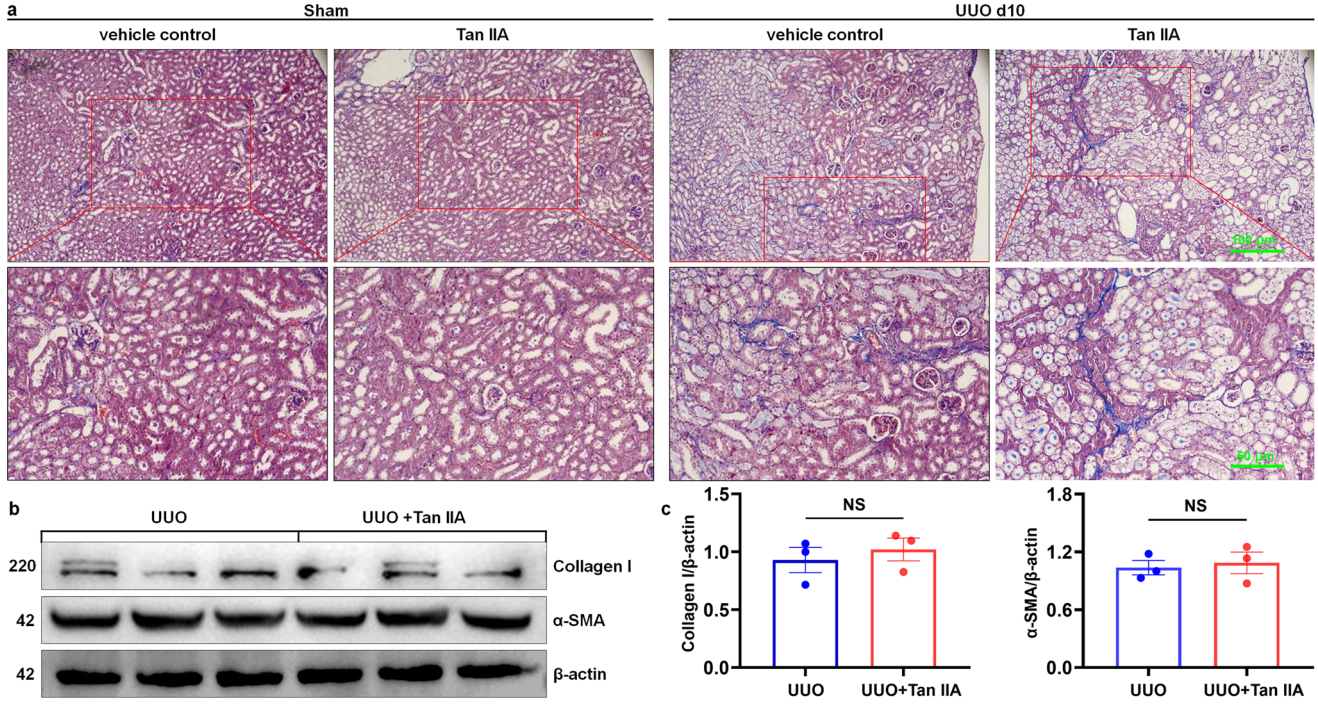

Figure 5. Tan IIA treatment did not improve UUO-induced renal fibrosis in GSDMD$^{-/-}$ mice.
UUO was induced in Gasdermin D (GSDMD)−/− mice, and kidney tissues were collected on day 10 after UUO surgery. (a) Representative microscopy images of Masson Trichrome (MT) staining in kidney sections of GSDMD knockout mice treated with Tan IIA or vehicle control. (b) Protein expression levels of α-SMA and collagen I in the UUO and UUO+Tan IIA groups. (c) Quantitative analysis of α-SMA and collagen I protein expressions in the UUO and UUO+Tan IIA groups. Data were analyzed using an unpaired t-test (n = 3).

Conclusions

Our research unveils a novel mechanism by which Tan IIA mitigates ureteral obstruction-induced nephropathy, specifically by inhibiting GSDMD-mediated pyroptosis. Following ureteral obstruction, the NLRP3-Caspase 1-GSDMD pathway is activated, resulting in pyroptosis in kidney tissue, the release of the inflammatory cytokine IL-1β, and the progression of renal fibrosis. Tan IIA effectively inhibits this pathway, reducing both pyroptosis and inflammation in RTECs and ultimately alleviating fibrosis. These findings demonstrate the therapeutic potential of Tan IIA in treating progressive obstructive nephropathy by modulating pyroptosis. Nevertheless, it is essential to recognize that other cell death pathways may also contribute to the anti-fibrotic effects of Tan IIA, which warrants further investigation.

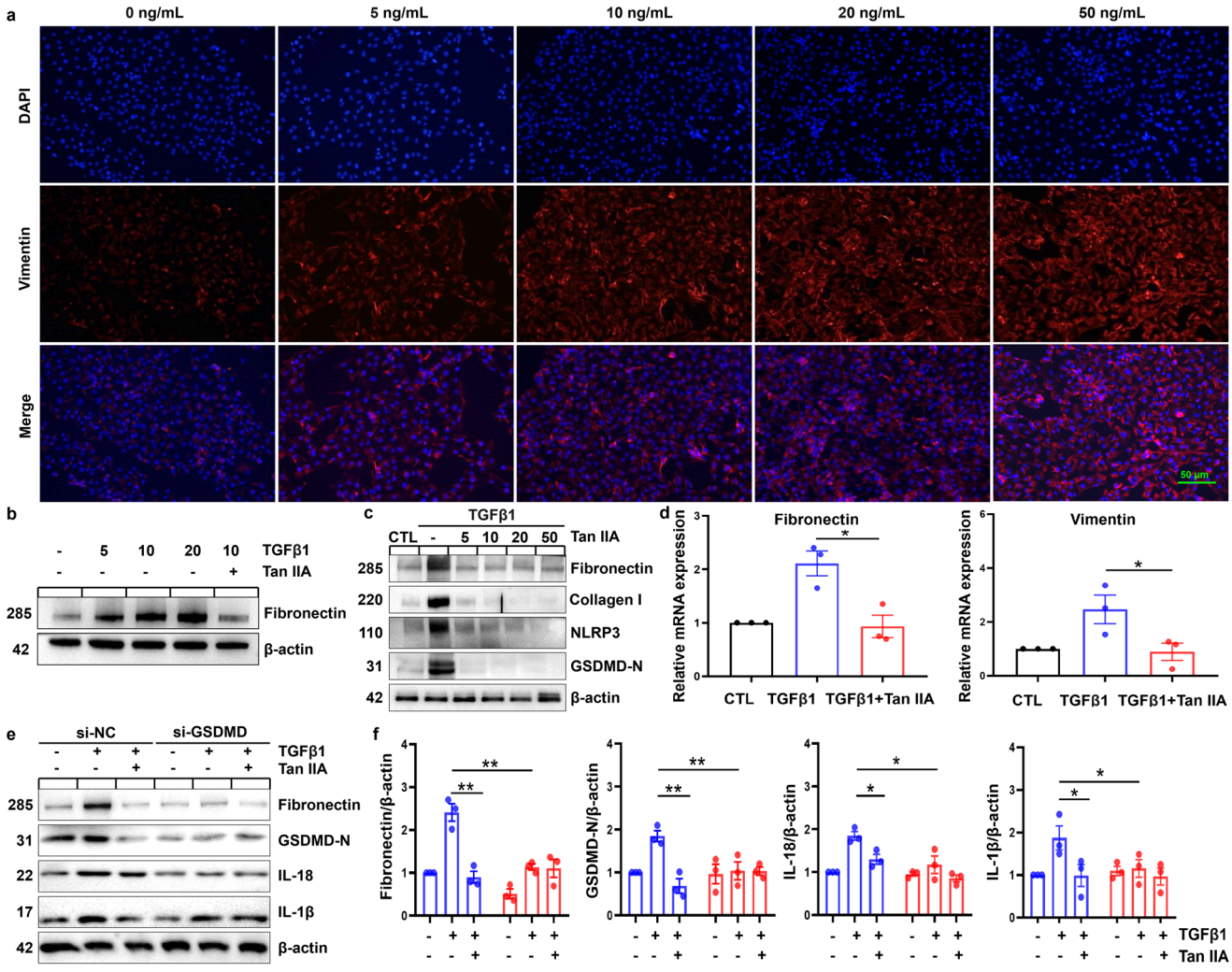

Figure 6. Tan IIA inhibited cell pyroptosis and reduced the production of fibrotic markers in RTECs.
Tan IIA inhibited the expression of profibrotic proteins in TGF-β1-stimulated HK-2 cells. (a) Immunofluorescence analysis using an anti-vimentin antibody in HK-2 cells treated with varying concentrations of TGF-β1 (0–50 ng/mL) for 24 h. (b) Protein expression levels of fibronectin in HK-2 cells treated with different concentrations of TGF-β1 (0–20 ng/mL) for 24 h. (c) Protein levels of fibronectin, collagen I, NLRP3, and GSDMD-N in TGF-β1-pretreated HK-2 cells following Tan IIA treatment at various concentrations (0–50 μM). (d) mRNA expression levels of vimentin and fibronectin in the control, TGF-β1, and Tan IIA + TGF-β1 groups. Data were analyzed using one-way ANOVA (3 independent experiments). *$p < 0.05$; **$p < 0.01$. (e) Protein levels of fibronectin, GSDMD-N, IL-18, and IL-1β in HK-2 cells induced with TGF-β1 (10 ng/mL) and pretreated with Tan IIA (5 μM) in different groups. (f) Quantitative analysis of fibronectin, GSDMD-N, IL-18, and IL-1β protein expressions in the different groups. Data were analyzed using two-way ANOVA (3 independent experiments). *$p < 0.05$; **$p < 0.01$.

Acknowledgment

We thank Prof. Limin Lu, from Fudan University for providing the GSDMD$^{-/-}$ mice.

Authors' contributions

CRediT: **Xueling Yang**: Data curation, Formal analysis, Investigation, Methodology, Project administration, Writing – original draft, Writing – review & editing; **Qinglin Luo**: Investigation, Methodology; **Zhifen Wu**: Methodology; **Chunxuan Wang**: Methodology; **Yuanjing Yang**: Methodology; **Luquan Zheng**: Methodology; **Ke Li**: Conceptualization, Writing – original draft, Writing – review & editing; **Lei Zhao**: Conceptualization; **Yang Jurong**: Conceptualization, Funding acquisition, Writing – original draft, Writing – review & editing.

Disclosure statement

No potential conflict of interest was reported by the author(s).

Funding

This work was supported by the National Natural Science Foundation of China (No. 82270723, 81770682), Natural Science Foundation of Chongqing (No. CSTB2024NSCQ-MSX0323) and the Chongqing Talent Program Project (cstc2021ycjh-bgzxm0090).

Data availability statement

Data supporting the findings presented are available from the corresponding author if requested.

References

Aglietti RA, Dueber EC. 2017. Recent insights into the molecular mechanisms underlying pyroptosis and Gasdermin family functions. Trends Immunol. 38(4):261–271. doi: 10.1016/j.it.2017.01.003.

Ansari MA, Khan FB, Safdari HA, Almatroudi A, Alzohairy MA, Safdari M, Amirizadeh M, Rehman S, Equbal MJ, Hoque M. 2021. Prospective therapeutic potential of Tanshinone IIA: an updated overview. Pharmacol Res. 164:105364. doi: 10.1016/j.phrs.2020.105364.

Baatarjav C, Komada T, Karasawa T, Yamada N, Sampilvanjil A, Matsumura T, Takahashi M. 2022. dsDNA-induced AIM2 pyroptosis halts aberrant inflammation during rhabdomyolysis-induced acute kidney injury. Cell Death Differ. 29(12):2487–2502. doi: 10.1038/s41418-022-01033-9.

Cao L, Huang B, Fu X, Yang J, Lin Y, Lin F. 2017. Effects of tanshinone IIA on the regulation of renal proximal tubular fibrosis. Mol Med Rep. 15(6):4247–4252. doi: 10.3892/mmr.2017.6498.

Cao G, Miao H, Wang YN, Chen DQ, Wu XQ, Chen L, Guo Y, Zou L, Vaziri ND, Li P, et al. 2022. Intrarenal 1-methoxypyrene, an aryl hydrocarbon receptor agonist, mediates progressive tubulointerstitial fibrosis in mice. Acta Pharmacol Sin. 43(11):2929–2945. doi: 10.1038/s41401-022-00914-6.

Chai R, Ye Z, Xue W, Shi S, Wei Y, Hu Y, Wu H. 2023. Tanshinone IIA inhibits cardiomyocyte pyroptosis through TLR4/NF-κB p65 pathway after acute myocardial infarction. Front Cell Dev Biol. 11:1252942. doi: 10.3389/fcell.2023.1252942.

Chang YT, Chung MC, Chang CH, Chiu KH, Shieh JJ, Wu MJ. 2022. Anti-EMT and anti-fibrosis effects of protocatechuic aldehyde in renal proximal tubular cells and the unilateral ureteral obstruction animal model. Pharm Biol. 60(1):1198–1206. doi: 10.1080/13880209.2022.2088809.

Chen F, Li S, Liu M, Qian C, Shang Z, Song X, Jiang W, Tu C. 2024. Targeting BRD4 mitigates hepatocellular lipotoxicity by suppressing the NLRP3 inflammasome activation and GSDMD-mediated hepatocyte pyroptosis. Cell Mol Life Sci. 81(1):295. doi: 10.1007/s00018-024-05328-7.

Coll RC, Schroder K, Pelegrín P. 2022. NLRP3 and pyroptosis blockers for treating inflammatory diseases. Trends Pharmacol Sci. 43(8):653–668. doi: 10.1016/j.tips.2022.04.003.

de Vasconcelos NM, Van Opdenbosch N, Van Gorp H, Parthoens E, Lamkanfi M. 2019. Single-cell analysis of pyroptosis dynamics reveals conserved GSDMD-mediated subcellular events that precede plasma membrane rupture. Cell Death Differ. 26(1):146–161. doi: 10.1038/s41418-018-0106-7.

Deng J, Tan W, Luo Q, Lin L, Zheng L, Yang J. 2021. Long non-coding RNA MEG3 promotes renal tubular epithelial cell pyroptosis by regulating the miR-18a-3p/GSDMD pathway in lipopolysaccharide-induced acute kidney injury. Front Physiol. 12:663216. doi: 10.3389/fphys.2021.663216.

Dou JY, Zhang M, Cen H, Chen YQ, Wu YF, Lu F, Zhou J, Liu XS, Gu YY. 2022. *Salvia miltiorrhiza* Bunge (Danshen) and bioactive compound tanshinone IIA alleviates cisplatin-induced acute kidney injury through regulating PXR/NF-κB signaling. Front Pharmacol. 13:860383. doi: 10.3389/fphar.2022.860383.

Dubyak GR, Miller BA, Pearlman E. 2023. Pyroptosis in neutrophils: multimodal integration of inflammasome and regulated cell death signaling pathways. Immunol Rev. 314(1):229–249. doi: 10.1111/imr.13186.

Elias EE, Lyons B, Muruve DA. 2023. Gasdermins and pyroptosis in the kidney. Nat Rev Nephrol. 19(5):337–350. doi: 10.1038/s41581-022-00662-0.

Fan Y, Yuan Y, Xiong M, Jin M, Zhang D, Yang D, Liu C, Petersen RB, Huang K, Peng A, et al. 2023. Tet1 deficiency exacerbates oxidative stress in acute kidney injury by regulating superoxide dismutase. Theranostics. 13(15):5348–5364. doi: 10.7150/thno.87416.

Fu H, Shen QR, Zhao Y, Ni M, Zhou CC, Chen JK, Chi C, Li DJ, Liang G, Shen FM. 2022. Activating α7nAChR ameliorates abdominal aortic aneurysm through inhibiting pyroptosis mediated by NLRP3 inflammasome. Acta Pharmacol Sin. 43(10):2585–2595. doi: 10.1038/s41401-022-00876-9.

Gao W, Wang X, Zhou Y, Wang X, Yu Y. 2022. Autophagy, ferroptosis, pyroptosis, and necroptosis in tumor immunotherapy. Signal Transduct Target Ther. 7(1):196. doi: 10.1038/s41392-022-01046-3.

Guo ZY, Wu X, Zhang SJ, Yang JH, Miao H, Zhao YY. 2025. *Poria cocos*: traditional uses, triterpenoid components and their renoprotective pharmacology. Acta Pharmacol Sin. 46(4):836–851. doi: 10.1038/s41401-024-01404-7.

He WT, Wan H, Hu L, Chen P, Wang X, Huang Z, Yang ZH, Zhong CQ, Han J. 2015. Gasdermin D is an executor of pyroptosis and required for interleukin-1β secretion. Cell Res. 25(12):1285–1298. doi: 10.1038/cr.2015.139.

Hu J, Gu W, Ma N, Fan X, Ci X. 2022. Leonurine alleviates ferroptosis in cisplatin-induced acute kidney injury by activating the Nrf2 signalling pathway. Br J Pharmacol. 179(15):3991–4009. doi: 10.1111/bph.15834.

Huang R, Fu P, Ma L. 2023. Kidney fibrosis: from mechanisms to therapeutic medicines. Signal Transduct Target Ther. 8(1):129. doi: 10.1038/s41392-023-01379-7.

Jiang C, Shao Q, Jin B, Gong R, Zhang M, Xu B. 2015. Tanshinone IIA attenuates renal fibrosis after acute kidney injury in a mouse model through inhibition of fibrocytes recruitment. Biomed Res Int. 2015:867140–867110. doi: 10.1155/2015/867140.

Jiang C, Zhu W, Shao Q, Yan X, Jin B, Zhang M, Xu B. 2016. Tanshinone IIA protects against folic acid-induced acute kidney injury. Am J Chin Med. 44(4):737–753. doi: 10.1142/s0192415x16500403.

Jin X, Ma Y, Liu D, Huang Y. 2023. Role of pyroptosis in the pathogenesis and treatment of diseases. MedComm (2020). 4(3):e249. doi: 10.1002/mco2.249.

Kalantar-Zadeh K, Li PK. 2020. Strategies to prevent kidney disease and its progression. Nat Rev Nephrol. 16(3):129–130. doi: 10.1038/s41581-020-0253-1.

Krukowski H, Valkenburg S, Madella AM, Garssen J, van Bergenhenegouwen J, Overbeek SA, Huys GRB, Raes J, Glorieux G. 2023. Gut microbiome studies in CKD: opportunities, pitfalls and therapeutic potential. Nat Rev Nephrol. 19(2):87–101. doi: 10.1038/s41581-022-00647-z.

Kuang BC, Wang ZH, Hou SH, Zhang J, Wang MQ, Zhang JS, Sun KL, Ni HQ, Gong NQ. 2023. Methyl eugenol protects the kidney from oxidative damage in mice by blocking the Nrf2 nuclear export signal through activation of the AMPK/GSK3β axis. Acta Pharmacol Sin. 44(2):367–380. doi: 10.1038/s41401-022-00942-2.

Lan HY. 2022. Macrophage-myofibroblast transition in kidney disease. Integr Med Nephrol Androl. 9(1):12. doi: 10.4103/2773-0387.358225.

Li H, Duann P, Li Z, Zhou X, Ma J, Rovin BH, Lin PH. 2022. The cell membrane repair protein MG53 modulates transcription factor NF-κB signaling to control kidney fibrosis. Kidney Int. 101(1):119–130. doi: 10.1016/j.kint.2021.09.027.

Li J, Huang X, He K, Wu S. 2023. The kidney antifibrotic effects of 5,7,3',4',5'-pentamethoxyflavone from *Bauhinia championii* in streptozotocin-induced diabetic rats: in vivo and in vitro experiments. Pharm Biol. 61(1):938–948. doi: 10.1080/13880209.2023.2222773.

Li K, Wu KY, Wu W, Wang N, Zhang T, Choudhry N, Song Y, Farrar CA, Ma L, Wei LL, et al. 2017. C5aR1 promotes acute pyelonephritis induced by uropathogenic *E. coli*. JCI Insight. 2(24):e97626. doi: 10.1172/jci.insight.97626.

Li S, Yang K, Cao W, Guo R, Liu Z, Zhang J, Fan A, Huang Y, Ma C, Li L, et al. 2023. Tanshinone IIA enhances the therapeutic efficacy of mesenchymal stem cells derived exosomes in myocardial ischemia/reperfusion injury via up-regulating miR-223-5p. J Control Release. 358:13–26. doi: 10.1016/j.jconrel.2023.04.014.

Li Y, Fu Y, Sun J, Shen J, Liu F, Ning B, Lu Z, Wei L, Jiang X. 2022. Tanshinone IIA alleviates NLRP3 inflammasome-mediated pyroptosis in Mycobacterium tuberculosis-(H37Ra-) infected macrophages by inhibiting endoplasmic reticulum stress. J Ethnopharmacol. 282:114595. doi: 10.1016/j.jep.2021.114595.

Li Y, Yuan Y, Huang ZX, Chen H, Lan R, Wang Z, Lai K, Chen H, Chen Z, Zou Z, et al. 2021. GSDME-mediated pyroptosis promotes inflammation and fibrosis in obstructive nephropathy. Cell Death Differ. 28(8):2333–2350. doi: 10.1038/s41418-021-00755-6.

Lin P, Qiu F, Wu M, Xu L, Huang D, Wang C, Yang X, Ye C. 2023. Salvianolic acid B attenuates tubulointerstitial fibrosis by inhibiting EZH2 to regulate the PTEN/Akt pathway. Pharm Biol. 61(1):23–29. doi: 10.1080/13880209.2022.2148169.

Liu Y, He M, Xiong H, Yuan F. 2022. Induction of pyroptosis in renal tubular epithelial cells using high glucose. Front Med (Lausanne). 9:874916. doi: 10.3389/fmed.2022.874916.

Ma FY, Tesch GH, Grynberg K, Ozols E, Mulley WR, Nikolic-Paterson DJ. 2023. A model of ischaemia-induced renal interstitial fibrosis in mice with established diabetes. Integr Med Nephrol Androl. 10(2):e00032. doi: 10.1097/IMNA-D-22-00032.

Miao H, Liu F, Wang YN, Yu XY, Zhuang S, Guo Y, Vaziri ND, Ma SX, Su W, Shang YQ, et al. 2024. Targeting *Lactobacillus johnsonii* to reverse chronic kidney disease. Signal Transduct Target Ther. 9(1):195. doi: 10.1038/s41392-024-01913-1.

Miao Q, Wang R, Sun X, Du S, Liu L. 2022. Combination of puerarin and tanshinone IIA alleviates ischaemic stroke injury in rats via activating the Nrf2/ARE signalling pathway. Pharm Biol. 60(1):1022–1031. doi: 10.1080/13880209.2022.2070221.

Nørregaard R, Mutsaers HAM, Frøkiær J, Kwon TH. 2023. Obstructive nephropathy and molecular pathophysiology of renal interstitial fibrosis. Physiol Rev. 103(4):2827–2872. doi: 10.1152/physrev.00027.2022.

Ren Q, Tao S, Guo F, Wang B, Yang L, Ma L, Fu P. 2021. Natural flavonol fisetin attenuated hyperuricemic nephropathy via inhibiting IL-6/JAK2/STAT3 and TGF-β/SMAD3 signaling. Phytomedicine. 87:153552. doi: 10.1016/j.phymed.2021.153552.

Roccatello D, Lan HY, Sciascia S, Sethi S, Fornoni A, Glassock R. 2024. From inflammation to renal fibrosis: a one-way road in autoimmunity? Autoimmun Rev. 23(4):103466. doi: 10.1016/j.autrev.2023.103466.

Ruiz-Ortega M, Rayego-Mateos S, Lamas S, Ortiz A, Rodrigues-Diez RR. 2020. Targeting the progression of chronic kidney disease. Nat Rev Nephrol. 16(5):269–288. doi: 10.1038/s41581-019-0248-y.

Sanz AB, Sanchez-Niño MD, Ramos AM, Ortiz A. 2023. Regulated cell death pathways in kidney disease. Nat Rev Nephrol. 19(5):281–299. doi: 10.1038/s41581-023-00694-0.

Shao YF, Tang BB, Ding YH, Fang CY, Hong L, Shao CX, Yang ZX, Qiu YP, Wang JC, Yang B, et al. 2023. Kaempferide ameliorates cisplatin-induced nephrotoxicity via inhibiting oxidative stress and inducing autophagy. Acta Pharmacol Sin. 44(7):1442–1454. doi: 10.1038/s41401-023-01051-4.

Shi J, Gao W, Shao F. 2017. Pyroptosis: Gasdermin-mediated programmed necrotic cell death. Trends Biochem Sci. 42(4):245–254. doi: 10.1016/j.tibs.2016.10.004.

Song YQ, Lin WJ, Hu HJ, Wu SH, Jing L, Lu Q, Zhu W. 2023. Sodium tanshinone IIA sulfonate attenuates sepsis-associated brain injury via inhibiting NOD-like receptor 3/caspase-1/Gasdermin D-mediated pyroptosis. Int Immunopharmacol. 118:110111. doi: 10.1016/j.intimp.2023.110111.

Sun MY, Ye HJ, Zheng C, Jin ZJ, Yuan Y, Weng HB. 2023. Astragalin ameliorates renal injury in diabetic mice by modulating mitochondrial quality control via AMPK-dependent PGC1α pathway. Acta Pharmacol Sin. 44(8):1676–1686. doi: 10.1038/s41401-023-01064-z.

Tang PM, Nikolic-Paterson DJ, Lan HY. 2019. Macrophages: versatile players in renal inflammation and fibrosis. Nat Rev Nephrol. 15(3):144–158. doi: 10.1038/s41581-019-0110-2.

Wan J, Liu D, Pan S, Zhou S, Liu Z. 2022. NLRP3-mediated pyroptosis in diabetic nephropathy. Front Pharmacol. 13:998574. doi: 10.3389/fphar.2022.998574.

Wang B, Yang LN, Yang LT, Liang Y, Guo F, Fu P, Ma L. 2024. Fisetin ameliorates fibrotic kidney disease in mice via inhibiting ACSL4-mediated tubular ferroptosis. Acta Pharmacol Sin. 45(1):150–165. doi: 10.1038/s41401-023-01156-w.

Wang DT, Huang RH, Cheng X, Zhang ZH, Yang YJ, Lin X. 2015. Tanshinone IIA attenuates renal fibrosis and inflammation via altering expression of TGF-β/Smad and NF-κB signaling pathway in 5/6 nephrectomized rats. Int Immunopharmacol. 26(1):4–12. doi: 10.1016/j.intimp.2015.02.027.

Wang F, Huang M, Wang Y, Hong Y, Zang D, Yang C, Wu C, Zhu Q. 2022. Membrane attack complex C5b-9 promotes renal tubular epithelial cell pyroptosis in trichloroethylene-sensitized mice. Front Pharmacol. 13:877988. doi: 10.3389/fphar.2022.877988.

Wang H, Jiang Q, Zhang L. 2022. Baicalin protects against renal interstitial fibrosis in mice by inhibiting the TGF-β/Smad signalling pathway. Pharm Biol. 60(1):1407–1416. doi: 10.1080/13880209.2022.2097700.

Wang JL, Hua SN, Bao HJ, Yuan J, Zhao Y, Chen S. 2023. Pyroptosis and inflammasomes in cancer and inflammation. MedComm (2020). 4(5):e374. doi: 10.1002/mco2.374.

Wang Y, Li Y, Chen Z, Yuan Y, Su Q, Ye K, Chen C, Li G, Song Y, Chen H, et al. 2022. GSDMD-dependent neutrophil extracellular traps promote macrophage-to-myofibroblast transition and renal fibrosis in obstructive nephropathy. Cell Death Dis. 13(8):693. doi: 10.1038/s41419-022-05138-4.

Wang YN, Zhang ZH, Liu HJ, Guo ZY, Zou L, Zhang YM, Zhao YY. 2023. Integrative phosphatidylcholine metabolism through phospholipase A_2 in rats with chronic kidney disease. Acta Pharmacol Sin. 44(2):393–405. doi: 10.1038/s41401-022-00947-x.

Wozniak J, Floege J, Ostendorf T, Ludwig A. 2021. Key metalloproteinase-mediated pathways in the kidney. Nat Rev Nephrol. 17(8):513–527. doi: 10.1038/s41581-021-00415-5.

Wu J, Raman A, Coffey NJ, Sheng X, Wahba J, Seasock MJ, Ma Z, Beckerman P, Laczkó D, Palmer MB, et al. 2021. The key role of NLRP3 and STING in APOL1-associated podocytopathy. J Clin Invest. 131(20):e136329. doi: 10.1172/jci136329.

Wu M, Xia W, Jin Q, Zhou A, Wang Q, Li S, Huang S, Zhang A, Zhang Y, Li Y, et al. 2021. Gasdermin E deletion attenuates ureteral obstruction- and 5/6 nephrectomy-induced renal fibrosis and kidney dysfunction. Front Cell Dev Biol. 9:754134. doi: 10.3389/fcell.2021.754134.

Wu Q, Guan YB, Zhang KJ, Li L, Zhou Y. 2023. Tanshinone IIA mediates protection from diabetes kidney disease by inhibiting oxidative stress induced pyroptosis. J Ethnopharmacol. 316:116667. doi: 10.1016/j.jep.2023.116667.

Wu S, Lu D, Gajendran B, Hu Q, Zhang J, Wang S, Han M, Xu Y, Shen X. 2023. Tanshinone IIA ameliorates experimental diabetic cardiomyopathy by inhibiting endoplasmic reticulum stress in cardiomyocytes via SIRT1. Phytother Res. 37(8):3543–3558. doi: 10.1002/ptr.7831.

Xue Y, Enosi Tuipulotu D, Tan WH, Kay C, Man SM. 2019. Emerging activators and regulators of inflammasomes and pyroptosis. Trends Immunol. 40(11):1035–1052. doi: 10.1016/j.it.2019.09.005.

Yang C, Mu Y, Li S, Zhang Y, Liu X, Li J. 2023. Tanshinone IIA: a Chinese herbal ingredient for the treatment of atherosclerosis. Front Pharmacol. 14:1321880. doi: 10.3389/fphar.2023.1321880.

Yang F, Bettadapura SN, Smeltzer MS, Zhu H, Wang S. 2022. Pyroptosis and pyroptosis-inducing cancer drugs. Acta Pharmacol Sin. 43(10):2462–2473. doi: 10.1038/s41401-022-00887-6.

Yang JR, Yao FH, Zhang JG, Ji ZY, Li KL, Zhan J, Tong YN, Lin LR, He YN. 2014. Ischemia-reperfusion induces renal tubule pyroptosis via the CHOP-caspase-11 pathway. Am J Physiol Renal Physiol. 306(1):F75–84. doi: 10.1152/ajprenal.00117.2013.

Yuan Q, Tang B, Zhang C. 2022. Signaling pathways of chronic kidney diseases, implications for therapeutics. Signal Transduct Target Ther. 7(1):182. doi: 10.1038/s41392-022-01036-5.

Zhang J, Hu Y, Wang H, Hou J, Xiao W, Wen X, Wang T, Long P, Jiang H, Wang Z, et al. 2022. Advances in research on the protective mechanisms of traditional Chinese medicine (TCM) in myocardial ischaemia-reperfusion injury. Pharm Biol. 60(1):931–948. doi: 10.1080/13880209.2022.2063342.

Zhao M, Guo J, Gao QH, Wang H, Wang F, Wang ZR, Liu SJ, Deng YJ, Zhao ZW, Zhang YY, et al. 2023. Relationship between pyroptosis-mediated inflammation and the pathogenesis of prostate disease. Front Med (Lausanne). 10:1084129. doi: 10.3389/fmed.2023.1084129.

Zheng F, Ma L, Li X, Wang Z, Gao R, Peng C, Kang B, Wang Y, Luo T, Wu J, et al. 2022. Neutrophil extracellular traps induce glomerular endothelial cell dysfunction and pyroptosis in diabetic kidney disease. Diabetes. 71(12):2739–2750. doi: 10.2337/db22-0153.

Zou TF, Liu ZG, Cao PC, Zheng SH, Guo WT, Wang TX, Chen YL, Duan YJ, Li QS, Liao CZ, et al. 2023. Fisetin treatment alleviates kidney injury in mice with diabetes-exacerbated atherosclerosis through inhibiting CD36/fibrosis pathway. Acta Pharmacol Sin. 44(10):2065–2074. doi: 10.1038/s41401-023-01106-6.